

Sreekantha B. Jonnalagadda and Nageswara R. Gollapalli, *S. Afr. J. Chem.*, 2001, **54**, 41-59, <<http://journals.sabinet.co.za/sajchem/>>, <http://ejour.sabinet.co.za/images/ejour/chem/chem_v54_a2.pdf>. [formerly: Sreekantha B. Jonnalagadda and Nageswara R. Gollapalli, *S. Afr. J. Chem.*, 2001, **54**, 2. (19pp.), <http://ejour.sabinet.co.za/images/ejour/chem/chem_v54_a2.pdf>.]

RESEARCH ARTICLE

Nonlinear Kinetics and Mechanism of Nile Blue Reaction with Acidic Bromate and with Aqueous Bromine

Sreekantha B. Jonnalagadda* and Nageswara R. Gollapalli**

Department of Chemistry, University of Durban-Westville, Durban 4000, South Africa

Received 14 August 2000; Revised 16 February 2001; Accepted 20 February 2001

Abstract

Nile blue, a dye of the phenoxazine class follows complex kinetics during its reaction with bromate in acidic solutions. The reaction kinetics were investigated using photometric and potentiometric techniques and a stopped flow apparatus. Under excess acid and bromate concentration conditions, nile blue, (NB⁺) initially depletes very slowly. After an induction period, a swift reaction occurs. The overall reaction is NB⁺ + BrO₃⁻ react to P + CH₃COOH + H⁺ + Br⁻, where P is the de-ethylated N-oxide derivative of nile blue. The rapid kinetics of the reaction of bromine direct with nile blue were also reported. A 11-step mechanism, consistent with the overall reaction dynamics and supported by simulations, is described. The role of various bromo- and oxybromo-species is discussed.

Registry No. Nile blue 3625-57-8, Sodium bromate 7647-15-6

Keywords Nonlinear reaction, kinetics and mechanism, acidic bromate, nile blue oxidation, aqueous bromine.

* To whom correspondence should be addressed.

** Permanent address: Department of Inorganic & Nuclear Chemistry, Andhra University, Visakhapatnam, India.

1. Introduction

Phenoxazine dyes are extensively used as mordents to cotton and leather due to their stability; brilliant colours and fastness to light.¹ The bright colours associated with organic dyes are due to the presence of conjugated π -bonds. In organic dyes, where the conjugation is extensive, the energy needed to effect electron promotion from the highest occupied to the lowest unoccupied molecular orbital falls within the UV-Visible electromagnetic radiation range, hence the bright colours. The reactivity of the dyes under varied oxidative and reducing media is pivotal in their applications as dyes under hostile conditions.

In open systems, such as isothermal stirred flow reactors, temporal behaviour and bistability can be easily generated and sustained. The Belousov-Zhabotinsky (BZ) and Uncatalysed -Bromate-Oscillator (UBO) type reactions, although closed systems, exhibit oscillatory phenomena and spatial patterns due to the intricate mechanisms involving generation and consumption of various bromo-, oxybromo- and other organic intermediates during the reaction.²⁻⁴ Although, several new oscillatory systems have been designed based on the chemistry of BZ reactions, the role of bromide ion under various concentration conditions is still not completely understood.⁵ The relative importance of the bromination and oxidation rates by bromine and hypobromous acid differ with the reducing substrates.

In closed systems involving acidic bromate, unlike many phenol/aniline derivatives that exhibit periodic phenomena, some organic dyes follow intricate non-linear kinetics, but with no temporal behaviour. In this communication we present the experimental results of a study of such a reaction, i.e. the reaction between Nile blue and acidic bromate. Nile blue (NB⁺) is a water-soluble dye of phenoxazine class, that exhibits a sharp absorption peak in the visible region ($\lambda_{\text{max}} = 635 \text{ nm}$, $\epsilon = 3.3 \times 10^4 \text{ dm}^3 \text{ mol}^{-1} \text{ cm}^{-1}$) and with no shift due to variation in pH.

Earlier, we reported the kinetics and reaction mechanisms of acidic bromate with phenothiazine class of dyes, methylene blue and toluidine blue.^{6,7} Those reactions with appreciable initial rate, differ from the Nile blue reaction. Academic interest in the dynamics of Nile blue - acidic bromate reaction arises from the extremely slow depletion rate of Nile blue in the initial stages, which is followed by an abrupt fast depletion. In this communication, we report the complex mechanism of the reaction between Nile blue and bromate in acidic solutions, identify the relative importance of bromine and

hypobromous acid reactions during the oxidation, and comment on the role of the bromide ion.

2. Experimental

2.1. Reagents

All chemicals were of Analar grade and all the solutions were prepared in distilled water. Nile blue sulphate salt (Aldrich) was used as supplied. Sodium sulphate was used as neutral salt to adjust the ionic strength.

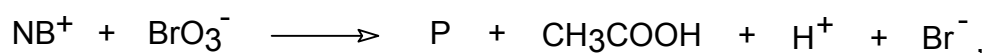
2.2. Kinetic Measurements

All the kinetics were conducted at $(25.0 \pm 0.1)^\circ\text{C}$ monitoring absorbance change (635 nm) using either the double mixing micro volume stopped-flow (Hi-Tech Scientific SF-61DX2) spectrophotometer or Cary II- Varian UV-Visible spectrophotometer. Always reaction was started by the addition and vigorous mixing of bromate to the mixture of other reagents. The Nile blue - aqueous bromine kinetics were investigated using a stopped-flow apparatus. Both the instruments were interfaced for data storage and have software to analyse the kinetic data. The overall potential was monitored by using the reference calomel/platinum electrodes with a data recording facility as function of time in a double walled thermostatted vessel $(25.0 \pm 0.1)^\circ\text{C}$.

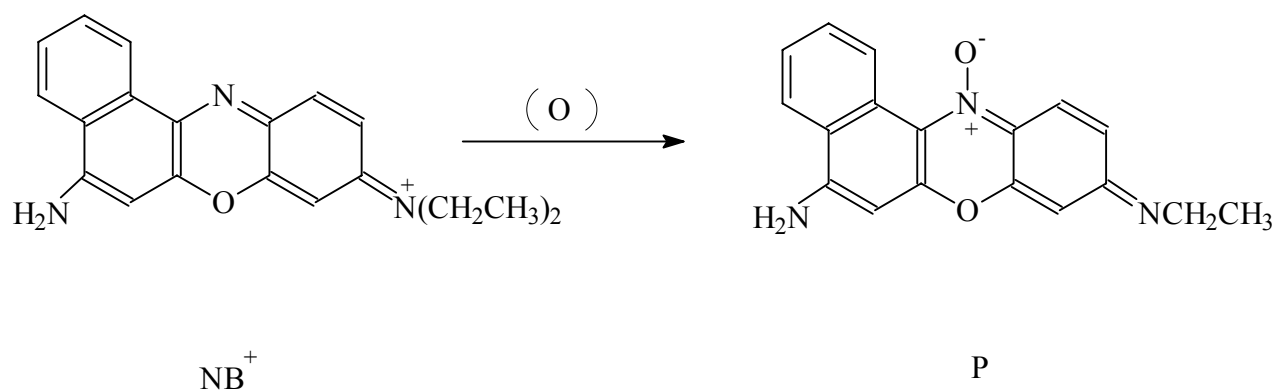
2.3. Stoichiometry and Product Analysis

For product analysis, Nile blue (200 mg in 250 ml of water), 3.0 mol dm^{-3} sulphuric acid (100 ml) and 0.1 mol dm^{-3} potassium bromate (150 ml) were mixed. After 24 hours, the organic components were extracted with ethyl acetate. The recrystallised reaction product was colourless. The mass spectrum of the sample gave m/z 305. Significant peaks m/z were observed at m/z 262, 246, 140 and 43, suggesting that the major oxidative product is the de-ethylated N-oxide derivative of Nile blue.⁸ N-oxide formation from oxidation of pyridines by hydrogen peroxide was reported in the literature⁹, as is formation of de-methylated products upon oxidation of phenothiazine dyes.⁶ TLC investigation of the reaction products using benzene and ethyl acetate in 2:1 ratio as eluent, with a reference standard showed the presence of acetic acid as an oxidation product. Studies on further characterisation of the reaction products are in progress. Using 1:20 and 1:50 molar ratios of $[\text{NB}^+]$: $[\text{BrO}_3^-]$ and excess of acid concentration, the

stoichiometric ratio was determined in triplicate runs. The residual bromate concentration was established iodometrically titrating with standard thiosulfate^{10, 11}. Under excess bromate conditions, Nile blue reacted with bromate in a 1:1 stoichiometric ratio within $\pm 10\%$ accuracy.



where P = de-ethylated N-oxide derivative of Nile blue.



3. Results and Discussion

Figure 1 illustrates 25 repetitive spectra of the Nile blue-acidic bromate reaction mixture, between 350 and 750 nm and scanned at 12 s intervals (scan speed 50 nm s^{-1}). Initial reactant concentrations were $[\text{NB}^+] = 1.0 \times 10^{-5} \text{ mol dm}^{-3}$, $[\text{H}^+] = 0.75 \text{ mol dm}^{-3}$ and $[\text{BrO}_3^-] = 5.0 \times 10^{-3} \text{ mol dm}^{-3}$. In the first 10 cycles, negligible changes occurred in the spectra. The 11th cycle shows the formation of a transient intermediate, which quickly disappears by the 12th cycle. By the completion of the 12th cycle, i.e. within 12 s, almost all the Nile blue was consumed. The depletion of NB^+ occurs very slowly in the initial stages, followed by a steep drop in its concentration. Figure 2a illustrates the profiles of typical Nile blue consumption kinetic curves (curves **a**, **b** & **c**) as function of bromate variation at constant ionic strength. Unlike other bromate systems, which display significant change in reductant concentration in the initial stages, the initial depletion of Nile blue was very slow. For each kinetic run, the *pseudo*-first-order rate constant (k') (ln absorbance versus time between 5 and 90 s) was determined. The ln abs. versus time plots were not ideal straight lines ($R^2 \geq 0.93$) (Figure 2b). The slopes from the duplicate runs had less than 5% deviation showing good reproducibility. The induction time (t_i) for the transition to rapid kinetics was estimated from the intersection of the tangents drawn to the sloping curves.

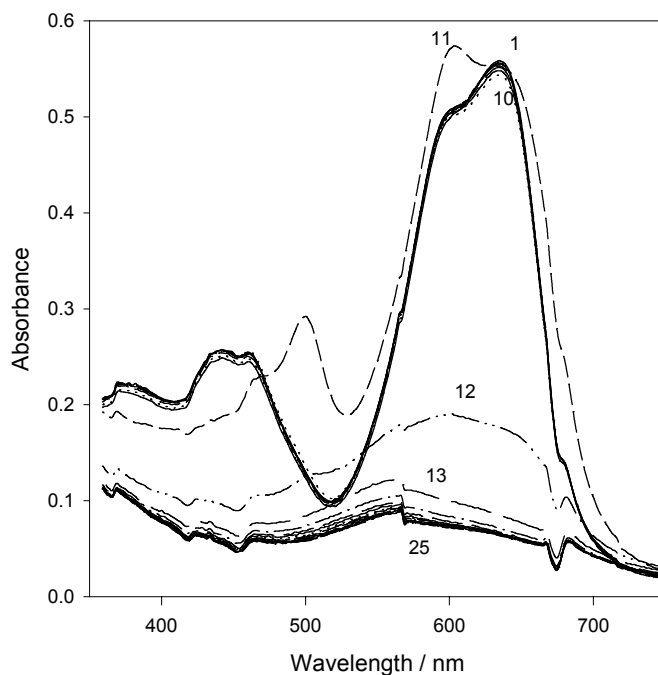


Figure 1 Repetitive spectra: Nile blue-acidic bromate reaction.
 $[NB^+] 1.0 \times 10^{-5} \text{ mol dm}^{-3}$, $[BrO_3^-] 5.0 \times 10^{-3} \text{ mol dm}^{-3}$ and $[H^+] = 0.75 \text{ mol dm}^{-3}$.
 Scan rate 12 s per cycle.

Considering the scope for spatial patterns in the unstirred systems, the effect of mild or occasional mixing of the solution during the reaction progress was investigated, and found to have no appreciable effect on the k' or I_t values. The mean values of k' from the duplicate runs are summarised in Table 1.

The k' versus $[BrO_3^-]$ plot was linear and passed through origin, which suggests that in the initial reaction rate has a first-order dependence on the bromate concentration. Linearity of the reciprocal I_t versus $[BrO_3^-]$ plot (Inset Figure 2) confirms that the reaction that influences the rapid kinetics has a first-order dependence on the bromate concentration. Furthermore, a positive x-intercept ($1.8 \times 10^{-3} \text{ mol dm}^{-3}$) of the plot suggests that a certain critical concentration of bromate is necessary for the transition to rapid kinetics. Thus, with $[BrO_3^-]_0$ equal or less than $1.8 \times 10^{-3} \text{ mol dm}^{-3}$, no rapid drop in the kinetic curve for Nile blue should occur. In the experiment with $[BrO_3^-]_0 = (2.0 \times 10^{-3} \text{ mol dm}^{-3})$, no rapid depletion of Nile blue was observed (in the first 40 minutes), confirming that its oxidation occurs through the slow path only.

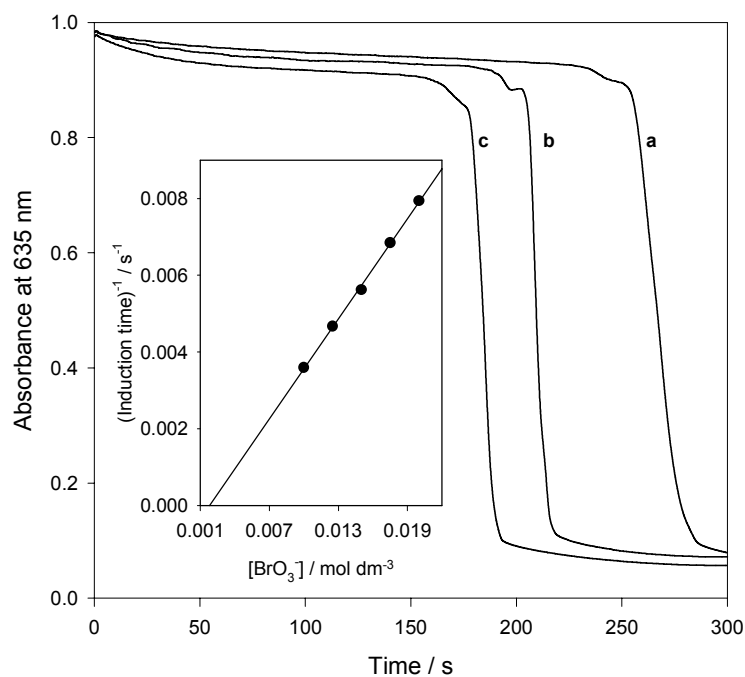


Figure 2a Kinetic curves - Effect of bromate variation
 $[\text{NB}^+] 3.0 \times 10^{-5} \text{ mol dm}^{-3}$, $[\text{H}^+] = 0.50 \text{ mol dm}^{-3}$ and $[\text{BrO}_3^-] / 10^{-2} \text{ mol dm}^{-3}$:
 Curve **a** = 1.00, **b** = 1.25 and **c** = 1.50. Inset: Plot of reciprocal induction time *versus* $[\text{BrO}_3^-]$.

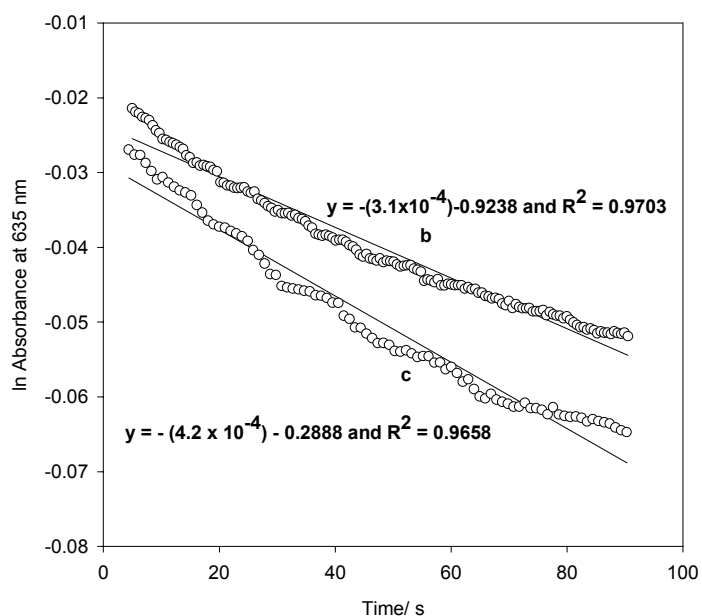


Figure 2b \ln absorbance *versus* time plots (5 to 90 s). (Conditions same as for Figure 2a- curves **b** and **c**).

Table 1 Effect of reactant concentrations on the kinetic curves.

[NB ⁺]	[BrO ₃ ⁻]	[H ⁺]	I	k'	K	I _t [*]	Reference to Figure & curve
/ 10 ⁻⁵ mol dm ⁻³	/ 10 ⁻² mol dm ⁻³	/ mol dm ⁻³	/ mol kg ⁻¹	/ 10 ⁻⁴ s ⁻¹ *	/ 10 ⁻² dm ⁶ mol ⁻² s ⁻¹	/ s	
3.0	1.00	0.50	1.52	2.6	5.20	278	Figure 2, curve a
3.0	1.25	0.50	1.52	3.1	4.96	217	2b
3.0	1.50	0.50	1.52	4.2	5.60	178	2c
3.0	1.75	0.50	1.52	4.5	5.14	146	
3.0	2.00	0.50	1.52	5.4	5.40	126	
3.0	1.25	0.50	2.71	3.1	4.96	217	Figure 3
3.0	1.25	0.60	2.71	3.9	5.20	132	Figure 3
3.0	1.25	0.70	2.71	4.6	5.26	92	Figure 3
3.0	1.25	0.80	2.71	5.2	5.20	79	Figure 3
3.0	1.25	0.90	2.71	6.4	5.68	59	Figure 3
1.0	1.25	0.50	1.51	3.2	5.12	574	
1.5	1.25	0.50	1.51	3.4	5.44	431	
2.0	1.25	0.50	1.51	3.5	5.60	316	
2.5	1.25	0.50	1.51	3.6	5.76	278	
3.0	1.25	0.50	1.51	3.6	5.76	215	

* Induction time; mean of duplicate runs with less than 5% deviation (Using the 5-90 minutes data, for the ln abs *versus* time plots R² varied between 0.93 to 0.97).

3.1. Dependence of Reaction Rate on Acid

The effect of [H⁺] on the reaction dynamics was studied at constant ionic strength (I = 1.52 mol kg⁻¹) (Table 1). Both the k' *versus* [H⁺] and the reciprocal I_t *versus* [H⁺] plots, which were straight lines suggest that the rates at the initial stage and of the rapid step have first-order dependence on H⁺ concentration. The x-intercept (0.10 mol dm⁻³) for the k' *versus* [H⁺] plot (Inset, Figure 3) suggests that for a given [BrO₃⁻], a threshold minimum [H⁺] is required for the reaction to occur. Such an intercept is expected, as BrO₃⁻ is known to be passive at pH > 4 and no reaction occurs.¹⁰ Further, a positive x-intercept = 0.35 mol dm⁻³, for the I_t⁻¹ *versus* [H⁺] plot (Figure 3) suggests that a minimum concentration of acid is required for the initial reaction's transition to rapid depletion. With [H⁺]₀ = 0.2 mol dm⁻³, the Nile blue depletion was slow throughout the reaction, as expected by the intercept. With [BrO₃⁻]₀ = 1.25 x 10⁻² mol dm⁻³ and [H⁺]₀ between 0.1

and 0.35 mol dm^{-3} , the oxidation of Nile Blue occurred through a slow reaction only.

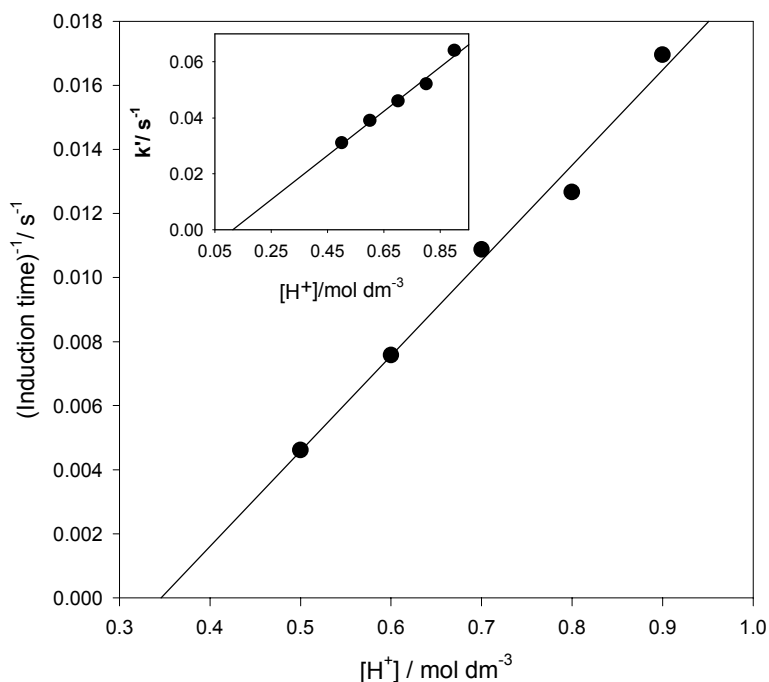


Figure 3 Effect of acid variation. $[\text{NB}^+] 3.0 \times 10^{-5} \text{ mol dm}^{-3}$ and $[\text{BrO}_3^-] 1.25 \times 10^{-2} \text{ mol dm}^{-3}$ and $[\text{H}^+] = 0.50\text{-}0.90 \text{ mol dm}^{-3}$. Plot of Reciprocal induction time *versus* $[\text{H}^+]$. Inset: Rate constant, k' *versus* $[\text{H}^+]$.

3.2. Dependence of Reaction Kinetics on Nile Blue Concentration

At excess concentrations of H^+ and BrO_3^- , the k' values remained unaltered with the variation of $[\text{NB}^+]$. The t_i^{-1} *versus* $[\text{NB}^+]$ plot gave a straight line passing through the origin confirming the first-order dependence of the initial reaction on the reducing substrate. The results for Nile Blue variation (Table 1, last five rows) show that induction time decreases with an increase in $[\text{NB}^+]$ confirming a direct reaction between NB^+ and BrO_3^- in acidic media.

3.3. Effect of Added Bromide on the Reaction

Figure 4 illustrates the profiles of absorbance *versus* time plots in the absence (curve **b**) and in the presence of KBr (curves **d** to **g**). An addition of $[\text{Br}^-]$ (5.0×10^{-7} - $5.0 \times 10^{-6} \text{ mol dm}^{-3}$), enhanced the rate of the initial depletion of NB^+ , but interestingly increased the induction times (curves **d**, **e** and **f**). A further addition of bromide ($>1.0 \times 10^{-5} \text{ mol dm}^{-3}$), resulted in a fast exponential decay of the Nile Blue and no transition to swift kinetics

was observed (curve **g**). Dual role of bromide ion as an inhibitor and auto-catalyst under low and high concentration conditions respectively was reported for the reactions of methyl orange with bromine¹² and of indigo carmine with acidic bromate¹³, but the mechanism was not explained.

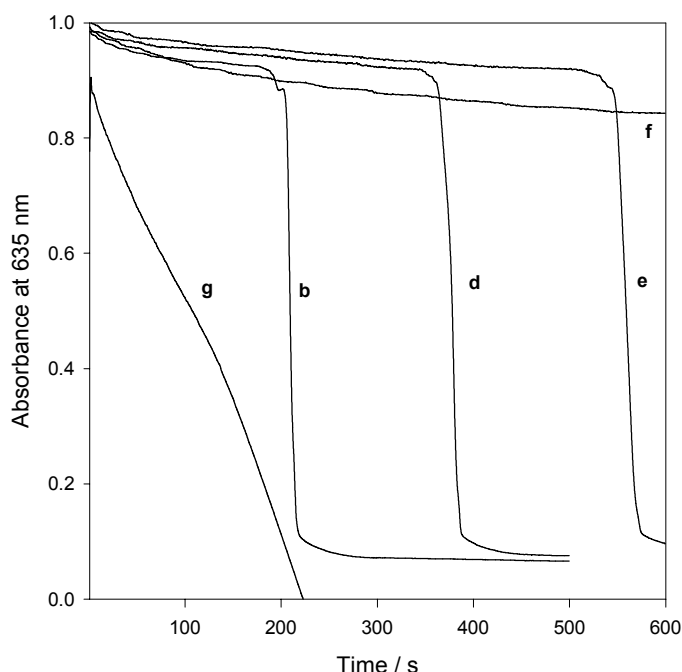


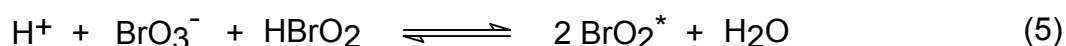
Figure 4 Effect of bromide on the depletion of NB^+ .
 $[\text{H}^+] 0.50 \text{ mol dm}^{-3}$, $[\text{BrO}_3^-] 1.25 \times 10^{-2} \text{ mol dm}^{-3}$ and $[\text{NB}^+] 3.0 \times 10^{-5} \text{ mol dm}^{-3}$.
 $[\text{Br}^-]/10^{-6} \text{ mol dm}^{-3}$: Curve **b** = Nil, **d** = 0.5, **e** = 1.0, **f** = 5.0 and **g** = 25.0.

At high concentrations, bromide reacts directly with acidic bromate generating HOBr and HBrO₂. A comparison the rate constant for the reaction with high $[\text{Br}^-]$ ($2.2 \text{ dm}^9 \text{ mol}^{-3} \text{ s}^{-1}$) (curve **g**) and the literature value for the Br^- - acidic bromate reaction ($2.5 \text{ dm}^9 \text{ mol}^{-3} \text{ s}^{-1}$, eq. 1) indicates that bromide-acidic bromate reaction dominants under high bromide conditions.. The mechanism of prolonged induction times with added bromide concentrations is still uncertain.

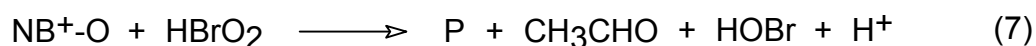
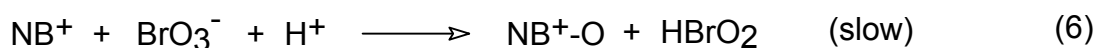
3.4. Reaction Mechanism

In the BZ type oscillatory chemical systems, Br^- acts as control intermediate, which switches between high and low concentration conditions. The drop from high $[\text{Br}^-]$ to low occurs through reaction of bromide with HBrO₂ and BrO_3^- . Regeneration of Br^- depends upon the nature of the organic species and its reaction rates with various oxybromo and bromo intermediates in the system. The crucial equations representing the chemistry of

bromo and oxybromo intermediates in the reactions of acidic bromate may be represented as follows:^{2,3}



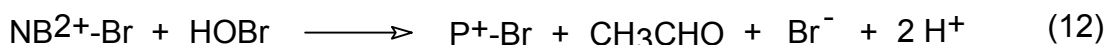
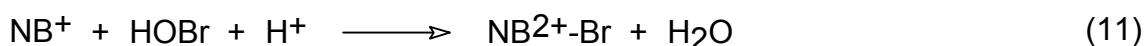
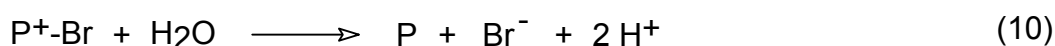
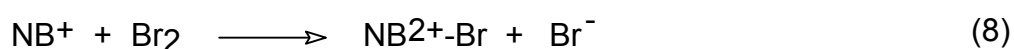
In Nile blue- acidic bromate reaction, in the absence of added bromide, the rate limiting step is direct reaction between NB^+ and BrO_3^- . The fast depletion step is the result of the rapid reaction of Nile blue with Br_2 and HOBr . The oxidation of Nile blue results in the formation of a transient intermediate, probably a N-oxide (NB^+-O), followed by a rapid de-ethylation resulting in formation of P (de-methylated N-oxide derivative Nile blue) and acetic acid. The positive charge on the nitrogen atom in the heterocyclic ring facilitates de-ethylation, and weakens the conjugated structure resulting in a colourless oxidation product.^{9, 14}



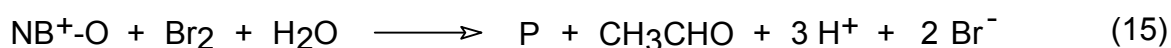
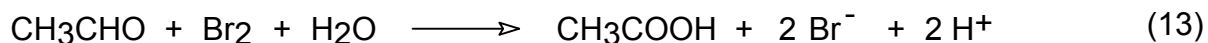
In the slow depletion stage, eq. 6 will be the rate-determining step. With $[\text{H}^+] = 0.5 \text{ mol dm}^{-3}$, $[\text{BrO}_3^-] = 1.5 \times 10^{-3} \text{ mol dm}^{-3}$ and $[\text{NB}^+] = 3 \times 10^{-5} \text{ mol dm}^{-3}$ and assuming the presence of $[\text{Br}^-] \leq 10^{-7} \text{ mol dm}^{-3}$ (an impurity with bromate), the forward rate of eq. 2, $(3.0 \times 10^6 [\text{H}^+] [\text{Br}^-] [\text{HBrO}_2] \text{ dm}^6 \text{ mol}^{-2} \text{ s}^{-1} = 3.0 \times 10^6 \times 0.5 \times 10^{-7} [\text{HBrO}_2] \text{ s}^{-1} = 0.15 [\text{HBrO}_2] \text{ s}^{-1})$ will be small compared with the forward rate of eq.3, $(3 \times 10^3 [\text{HBrO}_2]^2 \text{ dm}^3 \text{ mol}^{-1} \text{ s}^{-1})$. The increased concentration of HBrO_2 enhances its disproportionation rate and HOBr concentration, followed by an increase in Br^- concentration. With an increase in the concentration of bromide to a critical level, the reaction rate of HBrO_2 with bromide becomes appreciable (eq. 2), resulting in further increase in HOBr and Br_2 concentrations. Both bromine and hypobromous acid could react rapidly with NB^+ and other organic species. Relative levels of HOBr and Br_2 are controlled by the concentrations of H^+ and Br^- ions (eq. 4). The reaction of Br_2 with the organic moieties will increase $[\text{Br}^-]$, which is an auto-catalyst. Increase in Bromide ion concentration

exponentially increases the bromine production resulting in rapid depletion of the reducing substrate. Bromination of aromatic substrates and formation of bromo- or N-bromo- transient intermediates in oxidation reactions involving bromine are well known.¹⁵⁻¹⁸ The kinetics can be further complicated by the existence of a temporary sink for bromine, to delay the generation of bromide. The brominated species regenerate bromide upon further oxidation.^{16,17}

Taking into consideration, the long induction time and formation transient intermediate before the rapid depletion step (Fig.1), N-bromo species is proposed as an intermediate, for the reactions of bromine or hypobromous acid with NB⁺.



Other reactions important reactions are as follows:



To establish the roles of Br₂ and HOBr in the reaction mechanism, the kinetics of the fast reaction between Nile blue and aqueous bromine were studied by using the stopped flow apparatus. Due to very fast dynamics, the kinetics could be studied only with slightly excess bromine concentrations. Figure 5 illustrates the profiles of depletion of Nile blue under varied concentrations of acid (curves **h**, **i** & **j**) and alkali (curves **k** & **l**).

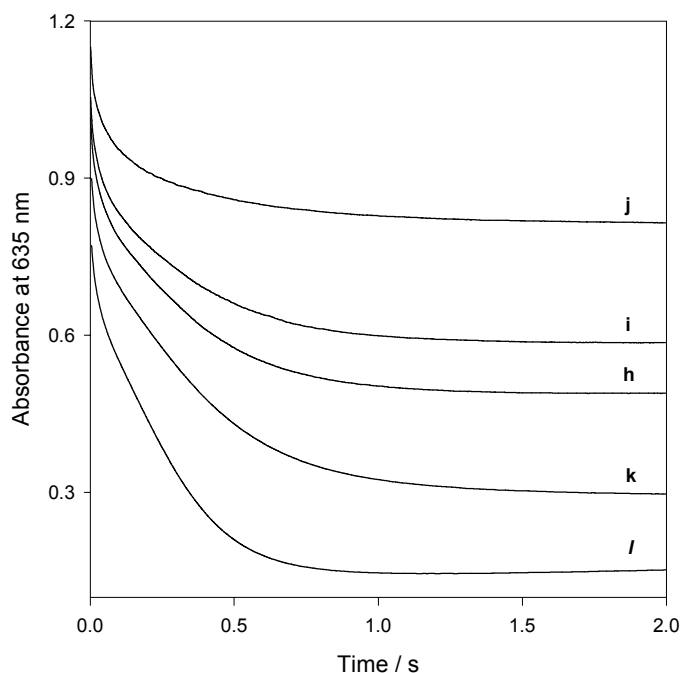


Figure 5 Nile blue - bromine reaction. Effect of added acid and base. $[NB^+] 3.0 \times 10^{-5} \text{ mol dm}^{-3}$. $[Br_2] = 2.88 \times 10^{-4} \text{ mol dm}^{-3}$: Curve **h** = $[H^+]$ or $[OH^-]$ Nil; **i** = $[H^+] 1.0 \times 10^{-5} \text{ mol dm}^{-3}$; **j** = $[H^+] 1.0 \times 10^{-4} \text{ mol dm}^{-3}$, **k** = $[OH^-] 2.0 \times 10^{-5} \text{ mol dm}^{-3}$ and **l** = $[OH^-] 1.0 \times 10^{-4} \text{ mol dm}^{-3}$.

For the reaction between Nile blue and aqueous bromine, kinetic curves had pseudo-first-order characteristics. Upon addition of acid or alkali, kinetic profiles were more complex. All the kinetic data had better fits with a bi-exponential equation ($y = A_1 \exp(-k_1 x) + A_2 \exp(-k_2 x) + Mx + C$), suggesting the simultaneous occurrence of two pseudo first-order reactions. Table 2 summarises the analysed results for the variation of concentrations of bromine, acid and alkali. With the increase in $[Br_2]$, k_1 value increased proportionately, while the other value decreased, indicating that first and second pseudo first-order rate coefficients evaluated correspond to the reaction of Nile blue with bromine (k'_{Br_2}) and hypobromous acid (k'_{HOBr}) respectively. The k'_{Br_2} value increased with an increase in added acid concentration, suggesting that oxidation of protonated Nile blue is faster than the unprotonated species. With an increase in added alkali concentration, k'_{Br_2} value decreased and k'_{HOBr} increased marginally. This could be possibly due to lowering of bromine concentration, which the shift in pH (refer eq. 4). Although hypobromous acid (HOBr) and hypobromite (OBr^-) concentrations increase with an increase in pH, hypobromite is less reactive than HOBr. Thus, k'_{HOBr} value is only marginally increased.

Table 2 Aqueous bromine-nile blue reaction.
 $[\text{NB}^+] = 3.0 \times 10^{-5} \text{ mol dm}^{-3}$

$[\text{Br}_2]$	$[\text{H}^+]$	$[\text{OH}^-]$	k'_{Br_2}	k'_{HOBr}	k_{Br_2}	k_{HOBr}	Refer to Figure & curve
$/10^{-4} \text{ mol dm}^{-3}$	$/10^{-5} \text{ mol dm}^{-3}$	$/10^{-5} \text{ mol dm}^{-3}$	$/\text{s}^{-1}$	$/\text{s}^{-1}$	$/10^4 \text{ dm}^3 \text{ mol}^{-1} \text{ s}^{-1}$	$/10^4 \text{ dm}^3 \text{ mol}^{-1} \text{ s}^{-1}$	
2.88			3.14 ± 0.06	3.13 ± 0.15	1.09		h
3.74			4.17 ± 0.09	0.72 ± 0.04	1.11		
4.32			4.61 ± 0.15	0.33 ± 0.02	1.07		
5.76			6.01 ± 0.02	0.036 ± 0.006	1.04		
2.88	1.0		3.46 ± 0.09	3.14 ± 0.19	1.20	1.09	i
2.88	5.0		12.81 ± 0.22	3.09 ± 0.04	4.45	1.07	
2.88	10.0		28.75 ± 0.59	3.02 ± 0.06	9.98	1.05	j
2.88		1.0	1.23 ± 0.08	2.62 ± 0.05		0.91	k
2.88		6.0	3.01 ± 0.04	0.262 ± 0.008		1.05	
2.88		10.0	0.064 ± 0.02	3.51 ± 0.05		1.22	l

Mean of 5 replicate runs with less than 3% std. deviation.

At high acid concentration all the nile blue is assumed protonated. Kinetics at high acid concentration could not be studied due limiting conditions for stopped flow apparatus to study very fast reactions. At high alkali concentrations, nile blue decolourises. Therefore studies on effect of alkali were restricted to low alkali additions only. Based on the results in Table 2, the second order rate constant for the reaction between protonated nile blue and bromine is taken as $1 \times 10^5 \text{ dm}^3 \text{ mol}^{-1}$ and for nile blue- HOBr reaction as $1 \times 10^4 \text{ dm}^3 \text{ mol}^{-1}$. The high rate coefficient for Br_2 , confirms the role of bromine as the reactive intermediate in the overall reaction. Thus under acidic conditions, HOBr is consumed through either conversion to bromine or oxidative reactions.

The changes in overall potential (emf) and $[\text{NB}^+]$ were monitored simultaneously in a continuously stirred system. Formation of bromine could not be monitored simultaneously due the overlap of the spectra of organic species at 390 nm. The emf change had three stages: an initial slow increase; a swift increase and again a slow increase (Fig. 6, curve b", concentrations as in curve b).

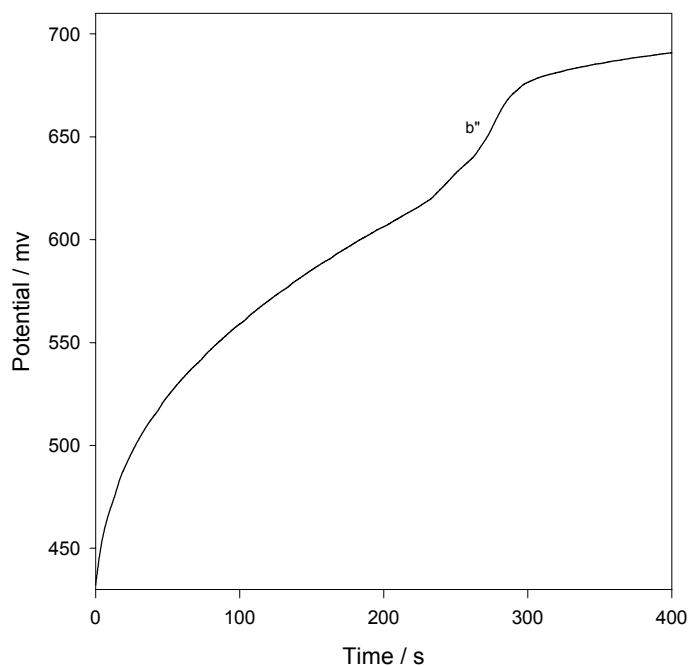


Figure 6 Overall potential versus time (Continuously stirred system). (Conditions as in Figure 2, curve **a**).

The first two stages could be due to the increasing levels of Br_2 or HOBr (redox potential of $\text{BrO}_3^- / \text{HOBr} = -1.49 \text{ V}$) followed by their consumption. A slow rise in the emf in the later part of the reaction occurred after the rapid depletion of NB^+ . This is due to the formation of Br_2 from the residual bromide, after consumption of the organic substrate. The redox potential for $\text{HOBr} / \text{Br}_2$ is -1.57 V and for $\text{Br}^- / \text{Br}_2$ is -1.09 V . In the continuously stirred systems, induction times were shorter than for the unstirred measurements. Under otherwise identical conditions, the unstirred reaction had an induction time of 214 s, in the continuously stirred system depletion occurred at 180 s.

3.5. Simulations

To compute the characteristic features of the reaction, i.e. very slow initial phase followed by an instantaneous reaction, simulations were executed using the semi-implicate Runge-Kutta method, which solves differential equations simultaneously.¹⁹ For the simulations, rate coefficients from literature values were used for eq. 1 to 5.¹⁹ Rate constants determined in the present studies were employed for eq. 6, 8 and 11. The rate coefficient for eq. 6 was crucial and rate limiting. Estimated rate constants were used for the remainder of the reactions. Estimated rate coefficients for reactions involving intermediates with bromo and oxybromo species were kept high, and values were

adjusted such that the simulated curves agreed with the experimental curves. Initially, computations were conducted using all the 15 proposed equations. To simplify the mechanism, less important equations were excluded by examining the response of simulations to the individual or set of reactions in a systematic way. Reaction steps, 5, 12, and 14 were found to be less significant. Furthermore, blocking eq. 11, i.e. reaction of HOBr with NB^+ had little effect on the simulated curve. Hence, the final simulations were carried out with the remaining 11 equations. Table 3 (see Appendix) summarises the elementary steps and rate coefficients used for the simulations. Figure 7 shows the experimental kinetic curve, **a** for Nile blue and corresponding simulated curve, **a'**. $[\text{NB}^+]$ in the simulated curve is the sum of the concentrations of residual NB^+ and the two proposed intermediates, N-oxide and N-Br. Based on the spectrum of the 11th cycle in Figure 1, for simplicity, the two intermediates, N-oxide and N-Br are assumed to absorb at the same wavelength and approximated to have same molar absorptivity.

The simulations could not entirely generate the sharp drop in Nile blue concentration, but the simulated curve gives nearly a good fit. Concentration curves for Br^- , Br_2 , HOBr and product were also simulated. The increase in the concentrations of Br_2 and HOBr in the simulated curves are fairly consistent with the expected increase in their concentrations based on the swift rise in emf immediately after the fast drop in Nile blue concentration (Figure 6). In the simulations at high $[\text{Br}^-]_0$, with an increase in bromide, the initial rates increased agreeing with the experiment curves. Although, at low $[\text{Br}^-]_0$, simulations were insensitive to its change, the experimentally observed prolonged induction times with increase in added $[\text{Br}^-]$ could not be simulated.

Figure 8 illustrates the three experimental curves and corresponding simulated curves for the variation of initial bromate. A good agreement in the induction times in the three sets of curves supports that proposed reaction scheme as the probable mechanism to explain the intricate reaction between Nile blue and acidic bromate. The simulations also support the assumption that under low pH conditions, Br_2 is the crucial reactive intermediate to drive the rapid dynamics, than HOBr. The appearance of Br_2 in the simulation after the depletion of organic substrate further confirms that the bromine is the reactive intermediate and is maintained at steady state in equilibrium with HOBr.

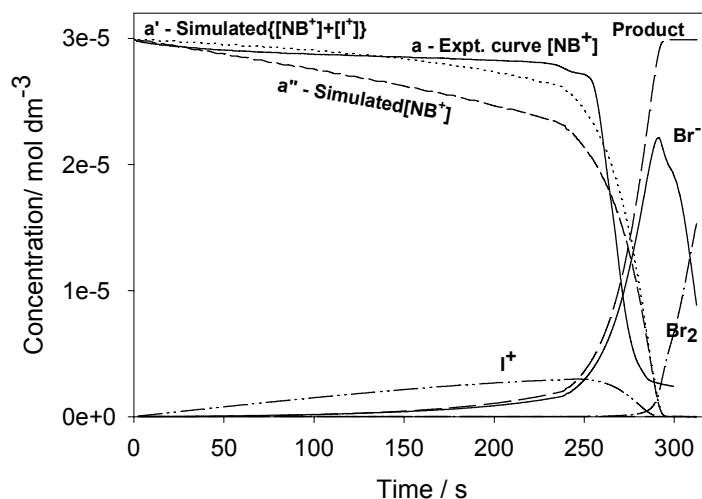


Figure 7 Simulations. (Conditions as in Figure 2, Curve **a**).
 $[NB^+] 3.0 \times 10^{-5} \text{ mol dm}^{-3}$, $[H^+] = 0.50 \text{ mol dm}^{-3}$ and $[BrO_3^-] 1.0 \times 10^{-2} \text{ mol dm}^{-3}$.
 Curve **a** - Experimental kinetic curve for NB^+ , **a'** - simulated curve for $[NB^+ + I^+]$, **a''** - simulated curve for NB^+ and simulated curves for I^+ , Br^- , Br_2 and P as marked.

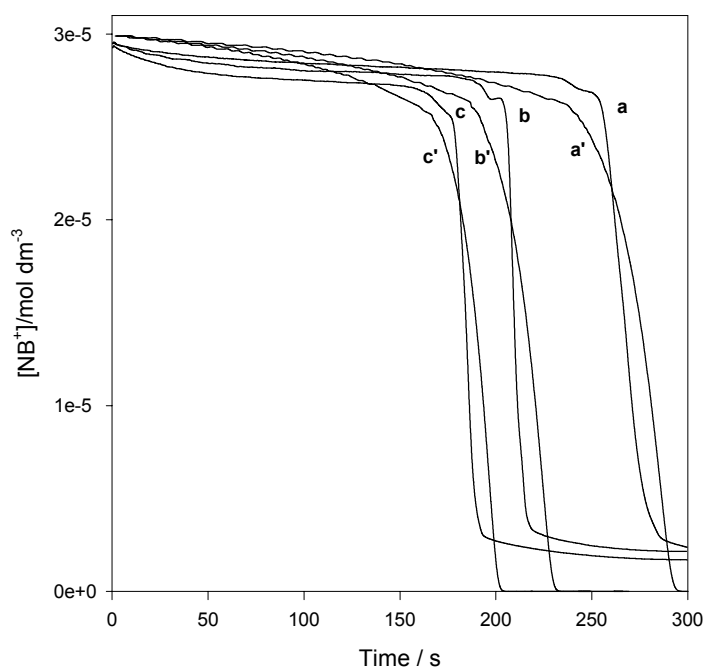


Figure 8 Simulations with different initial concentrations of bromate ion.
 Nile blue concentration *versus* time curves (Conditions as in Figure 2).
a, **b**, **c** are experimental curves. **a'**, **b'** and **c'** are simulated curves.

This kinetic study, elucidates the complex chemistry of nile blue-acidic bromate reaction. Unlike the other organic dyes, the resistance of nile blue to oxidation by acidic bromate is the cause of very slow reaction observed in the initial stages. The simulated

curves further support the experimentally predicted dominant role of bromine over hypobromous acid in the reaction. Further, the observed enormity in the rates of depletion of Nile blue in the rapid stage with acidic bromate and in the initial stages with high $[\text{Br}^-]_0$ also confirm the probable role of bromide ion as the autocatalyst and responsible for the rapid consumption of the dye after the induction time. More insight and understanding is needed to fully explain the dual role of bromide ion in the reaction mechanism, particularly the inhibitory phenomena of increased induction time with increased initial bromide.

Acknowledgements

The authors acknowledge the financial support received from the University of Durban-Westville, and National Research Foundation, Pretoria, South Africa.

References

- 1 M. Satake and T. Mido, *Chemistry of Colour*, Discovery Publishing House, New Delhi, 1995.
- 2 X. Y. Zhang and R. J. Field, *J. Phys. Chem.*, 1992, **96**, 1224.
- 3 H. Foersterling and M. Varga, *J. Phys. Chem.*, 1993, **97**, 7932.
- 4 K. Kurin-Csorgei, A. M. Zhabotinsky, M. Orban and I. R. Epstein, *J. Phys. Chem.*, 1996, **100**, 1593.
- 5 R. H. Simoyi, I. R. Epstein and K. Kustin, *J. Phys. Chem.*, 1994, **98**, 551.
- 6 G. K. Muthakia and S. B. Jonnalagadda, *J. Phys. Chem.*, 1989, **93**, 4751.
- 7 S. B. Jonnalagadda and N. Musengiwa, *Int. J. Chem. Kinet*, 1998, **30**, 111.
- 8 J. G. Grasselli and W. M. Ritchey, *Atlas of Spectral Data and Physical Constants for Organic Compounds*, 2nd ed., Vol. 1, CRC Press, Cleveland, Ohio, 1975.
- 9 L. A. Paquette, *Principles of Modern Heterocyclic Chemistry*, W.A. Benjamin Inc., New York, 1968.
- 10 J. C. Sullivan and R. C. Thompson, *J. Inorg. Chem.*, 1979, **18**, 2375.
- 11 S. B. Jonnalagadda, *Internat. J. Chem. Kinetics.*, 1984, **16**, 1287.
- 12 R. A. Hasty, E. J. Lima and J. M. Ottaway, *Analyst*, 1981, **106**, 76.
- 13 S. B. Jonnalagadda, R. H. Simoyi and G. K. Muthakia, *J. Chem. Soc., Perkin Trans 2*, 1988, 1111.

- 14 R. C. Elderfield, *Heterocyclic Compounds*, Vol. 6, 2nd ed., Chapman and Hall, New York, 1957.
- 15 L. Gyorgyi, M. Varga, E. Koros, R. J. Field and P. Ruoff, *J. Phys. Chem.*, 1989, **93**, 2836.
- 16 I. Szalai and E. Koros, *J. Phys. Chem.*, 1998, **102**, 6892.
- 17 A. Granzow, W. Abraham and R. Fausto, Jr., *J. Am. Chem. Soc.*, 1974, **96**, 2454.
- 18 J. J. Harrison, J. P. Pellegrini and C. M. Selwitz, *J. Org. Chem.*, 1981, **41**, 2169.
- 19 P. Kaps and P. Rentdrop, *Numer. Math.*, 1979, **33**, 55.

Appendix

Table 3 Equations and rate coefficients used in simulations.

Eq. No ^a	Reaction	Rate coefficients	
		Forward reaction	Reverse reaction
1. ^b	$2 \text{H}^+ + \text{Br}^- + \text{BrO}_3^- \rightleftharpoons \text{HOBr} + \text{HBrO}_2$	$k_1 = 2.5 \text{ dm}^9 \text{ mol}^{-3} \text{ s}^{-1}$	$k_{-1} = 3.2 \text{ dm}^3 \text{ mol}^{-1} \text{ s}^{-1}$
2. ^b	$\text{H}^+ + \text{HBrO}_2 \rightleftharpoons 2 \text{HOBr}$	$k_2 = 3 \times 10^6 \text{ dm}^6 \text{ mol}^{-2} \text{ s}^{-1}$	$k_{-2} = 2 \times 10^{-5} \text{ dm}^3 \text{ mol}^{-1} \text{ s}^{-1}$
3. ^b	$2 \text{HOBr} \rightleftharpoons \text{H}^+ + \text{HOBr} + \text{BrO}_3^-$	$k_3 = 3 \times 10^3 \text{ dm}^3 \text{ mol}^{-1} \text{ s}^{-1}$	$k_{-3} = 1 \times 10^{-8} \text{ dm}^6 \text{ mol}^{-2} \text{ s}^{-1}$
4. ^b	$\text{H}^+ + \text{Br}^- + \text{HOBr} \rightleftharpoons \text{Br}_2 + \text{H}_2\text{O}$	$k_4 = 8 \times 10^9 \text{ dm}^6 \text{ mol}^{-2} \text{ s}^{-1}$	$k_{-4} = 2 \times 10^{-5} \text{ s}^{-1}$
6. ^c	$\text{NB}^+ + \text{BrO}_3^- + \text{H}^+ \longrightarrow \text{NB}^+\text{-O} + \text{HBrO}_2$	$k_6 = 5.4 \times 10^{-2} \text{ dm}^6 \text{ mol}^{-2} \text{ s}^{-1}$	
7.	$\text{NB}^+\text{-O} + \text{HBrO}_2 \longrightarrow \text{P} + \text{CH}_3\text{CHO} + \text{HOBr} + \text{H}^+$	$k_7 = 2.0 \times 10^4 \text{ dm}^3 \text{ mol}^{-1} \text{ s}^{-1}$	
8. ^c	$\text{NB}^+ + \text{Br}_2 \longrightarrow \text{NB}^{2+}\text{-Br} + \text{Br}^-$	$k_8 = 1.0 \times 10^5 \text{ dm}^3 \text{ mol}^{-1} \text{ s}^{-1}$	
9.	$\text{NB}^{2+}\text{-Br} + \text{Br}_2 + \text{H}_2\text{O} \longrightarrow \text{P}^+\text{-Br} + \text{CH}_3\text{CHO} + 2 \text{Br}^- + 3 \text{H}^+$	$k_9 = 2.0 \times 10^6 \text{ dm}^3 \text{ mol}^{-1} \text{ s}^{-1}$	
10.	$\text{P}^+\text{-Br} + \text{H}_2\text{O} \longrightarrow \text{P} + \text{Br}^- + 2 \text{H}^+$	$k_{10} = 2.0 \times 10^5 \text{ s}^{-1}$	
13.	$\text{CH}_3\text{CHO} + \text{Br}_2 + \text{H}_2\text{O} \longrightarrow \text{CH}_3\text{COOH} + 2 \text{Br}^- + 2 \text{H}^+$	$k_{13} = 6 \times 10^3 \text{ dm}^3 \text{ mol}^{-1} \text{ s}^{-1}$	
15.	$\text{NB}^+\text{-O} + \text{Br}_2 + \text{H}_2\text{O} \longrightarrow \text{P} + \text{CH}_3\text{CHO} + 3 \text{H}^+ + 2 \text{Br}^-$	$k_{15} = 2.0 \times 10^5 \text{ dm}^3 \text{ mol}^{-1} \text{ s}^{-1}$	

^a - Equation numbers correspond to the equations in the text. ^b Literature values. ^c Experimental values.